6-hour observing interval) has been neglected, except as a contribution to the measurement error; in any event, the variation could not be distinguished from possible drifts in the relative phases of the two DSN receivers. The circularly polarized receiver levels were set to yield equal values for the linearly polarized received signal during periods of direct pointing toward Earth; the absence of significant circular polarization in the echo (except over Maxwell Montes) is taken as evidence that this procedure was valid. We believe that small delay differences in the 15-dB receiver attenuators, present during direct downlink but removed during reception of the echo, may be responsible for a bias of a few degrees of electrical phase deduced from the polarization rotation observed at small angles of incidence. In any event, we have increased all of the "raw" values of polarization angle, as obtained from the primary reference, by an estimated 2.7° of bias, in order to bring the average value of the observed polarization angles for reflection from the "normal" surface at 13.7° incidence to its anticipated theoretical value of −43.5° (this value is quite insensitive to the precise value of the dielectric constant at this low incidence, and these data provide our secondary reference).

8. J. D. Kraus, *Radio Astronomy* (Cygnus-Quasar, Powell, OH, 1986), pp. 4–14.
9. F. T. Ulaby, R. K. Moore, A. K. Fung, *Microwave Remote Sensing* (Artech House, Norwood, MA, 1982), vol. 2.
10. *Handbook of Chemistry and Physics* (Chemical Rubber Publishing, Cleveland, 1973), p. F-145; G. R. Olhoeft, in *Physical Properties of Rocks*, Y. S. Touloukian, W. R. Judd, R. F. Roy, Eds. (Hemisphere Publishing, New York, 1989), p. 257.
11. W. M. Becker and V. A. Johnson, in *Chemistry of Selenium, Tellurium, and Polonium*, K. W. Bagnall, Ed. (Elsevier, Amsterdam, 1966), chap. 3.
12. *Handbook of Chemistry and Physics* (Chemical Rubber Publishing, Cleveland, 1973), p. D-142.
13. A. Seiff *et al.*, *J. Geophys. Res.* **85**, 7903 (1980).
14. R. A. Brackett, B. A. Fegley Jr., R. E. Arvidson, *ibid.* **100**, 1553 (1995).
15. The "skin depth" represents the distance, *d*, into the conducting surface at which the penetrating electromagnetic wave is reduced to 1/*e* of its external value; it is given by (6)

$$d = \sqrt{\frac{2}{\omega\sigma}}$$

16. J. S. Kargel and J. S. Lewis, *Icarus* **105**, 6 (1993).
17. B. Hapke, *ibid.* **88**, 407 (1990).
18. J. A. Wood, in *Venus II*, S. Bougher, D. Hunten, R. Phillips, Eds. (Univ. of Arizona Press, Tucson, in press).
19. M. K. Shepard, R. E. Arvidson, R. A. Brackett, B. A. Fegley Jr., *Geophys. Res. Lett.* **21**, 469 (1994).

20. We thank the staff of the NASA DSN, as well as the dedicated engineers of the Jet Propulsion Laboratory (JPL) and Lockheed-Martin Aerospace, for their painstaking support in implementing this complex experiment. This work was supported under NASA grants NAGW-3787, NAGW-4351, and NAGW-3702 and JPL contracts 959490 and 957089.

11 December 1995; accepted 23 April 1996

High-Resolution Molecular Spectroscopy of van der Waals Clusters in Liquid Helium Droplets

Matthias Hartmann, Roger E. Miller,* J. Peter Toennies,†
Andrej F. Vilesov

Small van der Waals clusters of sulfur hexafluoride (SF_6) and mixed SF_6–rare gas clusters were prepared inside large droplets of helium-4, with each droplet consisting of about 4000 helium atoms. A diode laser was used to measure the high-resolution infrared spectra of these clusters in the vicinity of the ν_3 vibrational mode. In all cases rotational structure was observed, indicating that the embedded species rotate nearly freely, although they had been cooled to a temperature of 0.37 kelvin. The results indicate that helium droplets are probably superfluid and thereby provide a uniquely cold yet gentle matrix for high-resolution spectroscopy.

Spectroscopy has contributed greatly to our understanding of molecular behavior, but unfortunately many of the methods are ineffective when applied to complex molecules because of spectral congestion (vibrational and rotational) that blurs the details. For this reason, free jet expansions are widely used to simplify spectra by cooling molecules (*1*). Nevertheless, for large molecules the heat capacity may be so large that the cooling is incomplete. Although ultracold solid matrices (*2*) overcome this limitation, the matrix interactions can significantly perturb the spectrum (*2, 3*). From this point of view, liquid He would be the ideal matrix, except for the fact that the solvated molecules are quickly lost to the container walls (*4–6*). This problem can be overcome if the molecules are captured inside small droplets of liquid He, thus providing the needed isolation (*7–9*). Reported here are high-resolution spectra (0.01 cm^{-1}) of a number of He-solvated molecules, clusters, and van der Waals complexes that demonstrate that this is a viable approach for carrying out ultracold spectroscopy of large molecules. The results show that the solvent effects are weak yet interesting in their own right and that the solvated species are cooled to the temperature of the liquid droplets (0.37 K).

We have previously studied the case of a single SF_6 molecule in a He droplet (*9, 10*). We concluded that the molecule was solvated inside the droplet in a homogeneous environment, as deduced from mass spectrometer experiments (*11*) and predicted by theory (*12–14*). This is in contrast with the idea that the SF_6 molecule is positioned at an asymmetric surface site [this hypothesis was proposed earlier on the basis of low-resolution infrared studies (*8*)]. The vibrational hot bands of SF_6, which are observed even in the free jet expansion spectra (*15*), were completely absent in our spectrum, indicating that the cooling was complete. These results suggested that liquid He droplets may provide an ultracold, gentle matrix in which molecules are free to rotate and that the detailed rotational structure may provide insights into the interactions between the liquid He and the trapped molecule. We found from the rotational structure of the SF_6 spectrum that the temperature of the ^4He droplet was $T = 0.37$ K. Nevertheless, in considering the generality of the method, one might argue that the spherical symmetry of the SF_6 molecule is ideally suited to minimizing the interaction with the He and that this example may not be representative of the general case. Rather than switching to a different molecule to address this issue, we chose to study van der Waals complexes of SF_6, for example, the dimer of SF_6 which has been studied extensively in free jet expansions (*16, 17*) and at low resolution in liquid He (*8*).

The experimental apparatus used in the present study has been described previously (*9, 10*) (Fig. 1). We introduced SF_6 molecules into the He droplets using a "pick-up" method (*18*). Once formed, the droplets passed through a scattering chamber where the gas of interest, SF_6, was added at a known pressure, typically 10^{-5} mbar. The average number of molecules captured by the He droplet depends directly on this pressure (*19*). Upon capturing a hot SF_6 molecule, the droplet rapidly evaporates He atoms from its surface, and after approximately 10^{-6} s, the temperature returns to the initial droplet temperature, cooling the captured molecule. Of the ~4000 He atoms that make up the droplet (*20*), about 600 evaporate during the capture process (*19*).

The SF_6-containing He droplets were detected by electron impact ionization in a quadrupole mass spectrometer. By far the most probable event is ionization of a He atom in the droplet, followed by resonant charge transfer with neighboring atoms until the charge localizes on the SF_6 molecule (*11*). This charge localization usually results in the complete evaporation of the remaining He droplet, owing to the release of the large difference in the ionization energies of He and SF_6 to the cluster. The largest ion signals were observed at the mass of the major SF_6 ion fragment, namely, SF_5^+. A semiconductor diode laser was used to ex-

---

Max-Planck-Institut für Strömungsforschung, Bunsenstraße 10, D-37073 Göttingen, Germany.

*Permanent address: Department of Chemistry, University of North Carolina, Chapel Hill, NC 27599, USA.
†To whom correspondence should be addressed.

cite the ν_3 vibrational mode (near 946.5 cm^{-1}) of the SF_6 solvated in the droplet as it passed between the scattering chamber and the detector. The vibrationally excited molecule is rapidly quenched by interactions with the surrounding He, resulting in the evaporation of ~200 additional He atoms. This laser-induced decrease in the droplet size, as well as the corresponding recoil of the droplet, results in a depletion in the mass spectrometer signal of several percent, providing a monitor of the spectral absorption.

Clusters of more than one SF_6 molecule can be formed in the interior of the liquid He droplets by coagulation, if the pressure in the scattering chamber is increased so that more than one molecule is captured (*19*). Spectra of the SF_6 dimer, trimer, and tetramer in He (Fig. 2B) were compared with the spectrum of the gas-phase dimer obtained with a diode laser in a free jet expansion (Fig. 2A) (*17*). We were able to assign the spectral features in Fig. 2B to specific cluster sizes by observing their dependence on the pressure in the capture cell (*19*). The dependence of the depletion signal (I_k) measured with the laser frequency tuned to the various spectral features observed in Fig. 2 is shown in Fig. 3 as a function of SF_6 pressure in the scattering chamber. The probability of formation of a specific $(SF_6)_k$ cluster is given by the probability for independent capture of k SF_6 molecules, which is a Poisson distribution (*19*),

$$I_k = K_{k0}\frac{(n\cdot\sigma\cdot L)^k}{k!}\exp(-n\cdot\sigma\cdot L) \qquad (1)$$

where K_{k0} is an amplitude factor, n is the number density of the gas, σ is the capture cross section, and L is the length of the cell. The experimental data were fit by Eq. 1 with σ = 3900 Å^2. This corresponds to a He droplet containing ~4100 atoms, which is in good agreement with a more direct measurement (*20*).

The dimer spectrum shown in Fig. 2B consists of two bands, which result from a lifting of the ν_3 vibrational degeneracy (*16*, *17*) as a result of the resonant interaction between the vibration-induced dipoles of the two SF_6 molecules. The two bands correspond to the positioning of transition dipoles of the SF_6 molecules either parallel (‖) or perpendicular (⊥) to the intermolecular axis. The dipole-dipole coupling energy, μ^2/R^3 (where μ is the transition dipole moment and R is the internuclear distance), is much stronger than the interaction with the surrounding He atoms; therefore, the splitting is characteristic of the distance between the SF_6 molecules in the dimer. This expectation is confirmed by the good agreement of these data with the observed splitting in the gas-phase dimer (Fig. 2A and Table 1). The spectra of the dimer and trimer (Fig. 2B) show P, Q, and R branch structure that is only partly resolved. This is most clearly seen for the parallel dimer band, whereas in the perpendicular dimer band strong shifts of the individual K subbands make the P, Q, and R branches less distinct.

Comparison of the two sets of dimer spectra, namely, for the gas phase and in the He liquid, shows that the rotational constant B in the latter case is considerably smaller than in the former, presumably as a result of the solvent interactions, which reduce the line spacing to less than the apparent resolution of ~0.01 cm^{-1}. We have reported a similar effect for the SF_6 monomer (*10*). Here, we show that rotational structure can also be observed for a van der Waals complex in a matrix. The dimer and even the trimer rotate in liquid He, establishing that this phenomenon is not restricted to spherical molecules. Even the tetramer spectrum shows some rotational structure.

We investigated the versatility of the method by considering the formation of mixed complexes within the He droplets, for example, by adding a rare gas (RG) to the capture cell. The spectra of the SF_6-RG

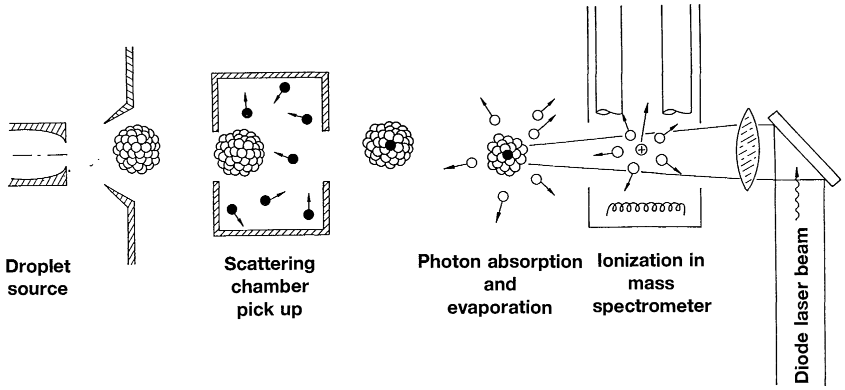

Fig. 1. Schematic diagram of the molecular beam apparatus for the depletion spectroscopy of molecules embedded in He droplets. The He droplets are produced by expansion of He gas from a cryogenically cooled orifice 5 μm in diameter at T_0 = 20 K and a pressure of P_0 = 44 bars. Under these conditions the He droplets are known to have a mean size of 4000 He atoms (*20*). The output (100 μW) of a continuous tunable diode laser (Mütek MSD 1100) interacts with the droplet beam as it passes from the scattering chamber to the detector. When the laser is in resonance with the molecules in the droplet, the absorbed energy leads to evaporation of ~200 He atoms and a depletion in the mass spectrometer signal. We measured the relative signal depletion by chopping the laser beam and using phase-sensitive detection.

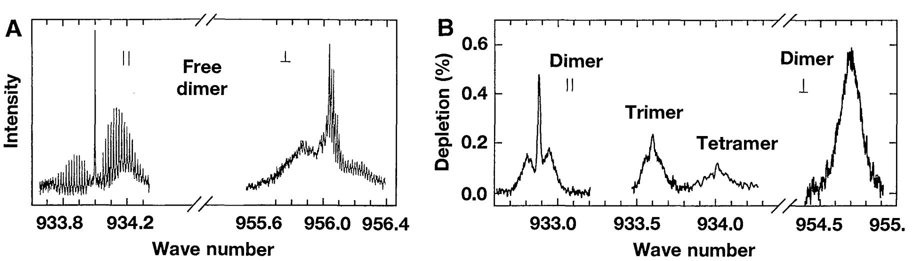

Fig. 2. Absorption spectra for $(SF_6)_n$. (**A**) Spectrum of SF_6 dimers in a free jet expansion obtained with a tunable diode laser (*17*). (**B**) Spectra obtained in the present work for $(SF_6)_n$ embedded in He droplets. The decrease in the relative absorption signal from dimer to tetramer is largely an artifact of the measuring method. The depletion is detected at the SF_5^+ mass in all cases. Because the number of fragmentation channels increases with cluster size, the signal is smaller for the larger clusters. ‖, dipole positioned parallel to the intermolecular axis; ⊥, dipole positioned perpendicular to the intermolecular axis.

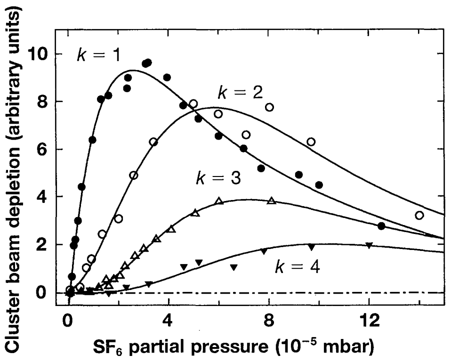

Fig. 3. Dependence of the depletion signal on the SF_6 pressure in the capture cell, as measured for the different bands of Fig. 2B. Solid curves are fits according to Eq. 1. Solid circle, monomer; open circle, dimer; open triangle, trimer; solid, inverted triangle, tetramer.

complexes (Fig. 4) also exhibit sharp lines and show rotational contours characteristic of the geometry of these complexes in the liquid. In these systems also, the spectra in the vicinity of the ν_3 vibrational mode are split into a parallel and a perpendicular band. However, for the SF_6-RG complexes this splitting is approximately one-fortieth of that for $(SF_6)_2$ (Table 1), as a result of the much weaker dipole-induced dipole interaction, $\alpha\mu/R^6$ (where α is the polarizability of the RG atom). In view of the much weaker coupling present in these spectra, it is likely that they are more sensitive to the solvent surroundings and might therefore provide detailed information on the interactions with the He environment. For the SF_6-Ne complex, no splitting was observed in the spectrum. A possible explanation for this behavior is that the surrounding He atoms compete with the Ne atom for occupancy of the first solvation shell around SF_6. As a result, the Ne atom no longer occupies a fixed site adjacent to SF_6 but rather on average is delocalized over the surface of the molecule. For the heavier RG atoms, the spectra indicate that the RG-SF_6 interaction is so much stronger than the He-SF_6 interaction that the RG-SF_6 structure is relatively unchanged from that of the gas phase.

Rotational constants *A* and *B* of the SF_6 dimer and those of the SF_6-RG complexes can be obtained from the detailed shape of the parallel bands, assuming $T = 0.37$ K (*10*). For the dimer we found $A = 0.007$ cm^{-1} and $B = 0.0044$ cm^{-1}, corresponding to rotation about the intermolecular bond axis and an axis perpendicular to this, respectively. Both of these values are much smaller than the corresponding constants for the free dimer, namely, $A = 0.0455$ cm^{-1} and $B = 0.0083$ cm^{-1} (*17*). For SF_6-Ar we find $A = 0.014$ cm^{-1} and $B = 0.0063$ cm^{-1}. The spectra of the free SF_6-Ar van der Waals complex are not known at present, and therefore we estimated the constants, assuming a rigid rotor with a bond distance of $R = 4.2$ Å, giving $A = 0.091$ cm^{-1} and $B = 0.023$ cm^{-1}. The large decrease in the rotational constants of the van der Waals complexes in He droplets corresponds to an increase in the moments of inertia. In (*10*) we showed that similar differences between the rotational constants of isolated and solvated SF_6 monomers could be explained by assuming that 8 He atoms are rigidly attached to the SF_6. For the dimer we found that ~30 attached He atoms are needed to fit both the *A* and the *B* constants. On the other hand, for SF_6-Ar, 16 and 30 rigidly attached He atoms are needed to explain *A* and *B*, respectively. We obtained these values by assuming that the He atoms are distributed on truncated spheres around both constituents of the complex with radii equal to the minima of the corresponding van der Waals potentials (*21*).

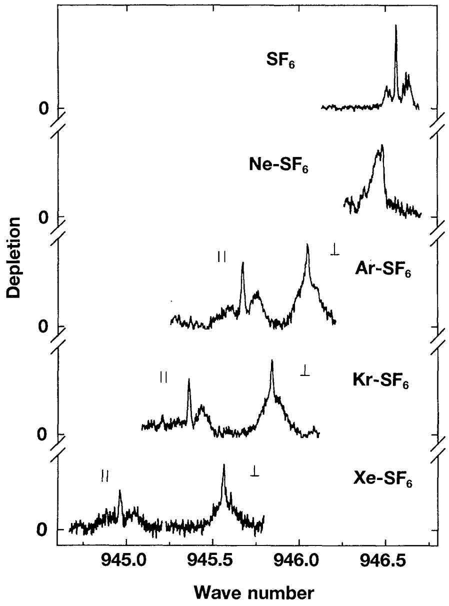

Fig. 4. Absorption spectra of the RG-SF_6 complexes compared with that of bare SF_6 in He droplets. The splitting in the RG-SF_6 spectra corresponds to the lifting of the ν_3 vibrational degeneracy as a result of the presence of the heavy RG atom.

The fact that different numbers of He atoms are needed to explain the two rotational constants of SF_6-Ar suggests that the assumption of rigidly attached He atoms may not be valid; rather, it is likely that the complexes have to push their way through the liquid, which is easier for rotation about the intermolecular axis of the prolate symmetric top than for rotation about the axis perpendicular to it. This behavior is indeed expected for the rotation of an anisotropic body in an ideal nondissipative liquid (*22*). The effective moment of inertia is increased simply by the backflow of the liquid displaced as the anisotropic body rotates. Such a model predicts a much greater effect on *B* than on *A*, as observed in the experiments. Of course, a more realistic theory must account for the strength of the interaction of the complexes with the He atoms relative to the He-He interaction. With increasing interaction strength, the motions of the body and medium cannot be separated and should be treated as a united quantum system.

Table 1. Band origins of the perpendicular (⊥) and parallel (‖) bands for $(SF_6)_2$ and SF_6-RG. The frequencies of the ν_3 vibrations of the free SF_6 monomer and SF_6 in a He droplet are 947.976 and 946.562 cm^{-1}, respectively.

Cluster in He droplet	ν (cm^{-1}) ‖ band	ν (cm^{-1}) ⊥ band
$(SF_6)_2$	932.88	954.70
Free $(SF_6)_2$*	934.007	956.098
SF_6-Ne	946.480†	
SF_6-Ar	945.673	946.049
SF_6-Kr	945.361	945.842
SF_6-Xe	944.962	945.564

*From (*17*). †Position of the sharp maximum.

The widths of the central Q branch lines give information on the rate of energy dissipation and thereby an upper bound on the shear viscosity of the surrounding He. From the relaxation lifetime and the moment of inertia determined for a single SF_6 molecule (*9*, *10*), and assuming a simple Stokes-Einstein model (*23*), we estimate an upper bound on the viscosity associated with its rotation of 0.08 micropoise (μP) (1 P = 1 dyne·s cm^{-2}). This is nearly three orders of magnitude smaller than the value of 30 μP for normal He (*24*). Although this model is quite crude, the large reduction in viscosity may be an indication that the He droplets are indeed superfluid. Our recent results on high-resolution laser electronic excitation of glyoxal in He droplets (*25*) provides independent evidence for superfluidity.

The spectroscopic experiments described here demonstrate that liquid He droplets can be used to prepare and study molecules and complexes at ultralow temperatures (a constant heat bath at 0.37 K) and at high resolution (0.01 cm^{-1}). The range of molecular "shapes" considered here suggests that the nearly free rotation of the molecules in liquid He is a general phenomenon. In all cases we observed very narrow vibrational bands indicative of long lifetimes, due to the weak interaction and the low temperature of the droplets. The very high resolution can be used to explore in great detail the interaction of the probe molecules with its superfluid environment.

Another advantage of this method is that it can easily be used to study complexes that cannot be prepared by other methods. Vibrational band origins of the complexes in He can be obtained with high precision. This method is potentially important for larger complexes where analysis of the rotational structure is less important and the main structural information comes from the analysis of vibrational spectral features. In the study of large molecules with low volatility, the method has the additional advantage that the pressure in the capture cell need only to be 10^{-5} mbar. This procedure may find use in the study of large biological molecules at these low temperatures, both isolated in the droplet and interacting with different numbers of water molecules that have also been captured by the droplet.

REFERENCES AND NOTES

1. D. H. Levy, *Annu. Rev. Phys. Chem.* **31**, 197 (1980).
2. Anonymous, *Chemistry and Physics of Matrix-Isolated Species* (Elsevier, Amsterdam, 1989).

3. B. I. Swanson and L. H. Jones, *J. Chem. Phys.* **74**, 3205 (1981).
4. E. B. Gordon *et al.*, *Chem. Phys.* **170**, 411 (1993).
5. G. zu Putlitz and M. R. Beau, in *Topics in Applied Physics*, vol. 70, M. Stuke, Ed. (Springer, Berlin, 1991), pp. 237–247.
6. I. F. Silvera, *Phys. Rev. B* **29**, 3899 (1984).
7. A. Scheidemann, J. P. Toennies, J. A. Northby, *Phys. Rev. Lett.* **64**, 1899 (1990).
8. S. Goyal, D. L. Schutt, G. Scoles, *ibid.* **69**, 933 (1992).
9. R. Fröchtenicht, J. P. Toennies, A. F. Vilesov, *Chem. Phys. Lett.* **229**, 1 (1994).
10. M. Hartmann, R. E. Miller, J. P. Toennies, A. F. Vilesov, *Phys. Rev. Lett.* **75**, 1566 (1995).
11. A. Scheidemann, B. Schilling, J. P. Toennies, *J. Phys. Chem.* **97**, 2128 (1993).
12. K. B. Whaley, *Int. Rev. Phys. Chem.* **13**, 41 (1994).
13. R. N. Barnett and K. B. Whaley, *J. Chem. Phys.* **99**, 9730 (1993).
14. F. Dalfovo, *Z. Phys. D Atoms Mol. Clusters* **29**, 61 (1994).
15. G. Schweizer, thesis, University of Bonn (1983).
16. J. Geraedts, M. Waayer, S. Stolte, J. Reuss, *Faraday Discuss. Chem. Soc.* **73**, 375 (1982).
17. R. D. Urban and M. Takami, *J. Chem. Phys.* **103**, 9132 (1995).
18. T. E. Gough, M. Mengel, P. A. Rowntree, G. J. Scoles, *Chem. Phys.* **83**, 4958 (1985).
19. M. Lewerenz, B. Schilling, J. P. Toennies, *J. Chem. Phys.* **102**, 8191 (1995).
20. ______, *Chem. Phys. Lett.* **206**, 381 (1993).
21. R. T. Pack, E. Piper, G. A. Pfeffer, J. P. Toennies, *J. Chem. Phys.* **80**, 4940 (1984), and references therein.
22. M. Lamb, *Hydrodynamics* (Cambridge Univ. Press, Cambridge, 1932), p. 152.
23. D. Kivelson, M. G. Kivelson, I. Oppenheim, *J. Chem. Phys.* **52**, 1810 (1970).
24. J. Wilks, *The Properties of Liquid and Solid Helium* (Clarendon, Oxford, 1967).
25. M. Hartmann, F. Mielke, J. P. Toennies, A. F. Vilesov, G. Benedek, in press.
26. We are grateful to R. Fröchtenicht for contributions in the early stages of this work and to M. Behrens for technical assistance. We also thank B. Whaley and M. Lewerenz for many valuable discussions and R. Dueren and U. Buck for technical support. M.H. and A.F.V. thank the Deutsche Forschungsgemeinschaft for financial support, and R.E.M. is grateful to the Alexander von Humboldt Society for a Senior Scientist award and to NSF (CHE-93-18936) for partial support.

4 January 1996; accepted 12 April 1996

Direct pH Measurement of NaCl-Bearing Fluid with an in Situ Sensor at 400°C and 40 Megapascals

Kang Ding* and William E. Seyfried Jr.

The pH of concentrated NaCl-HCl fluids (0.57 mole of NaCl per kilogram of water) has been measured at supercritical conditions of water with a yttria-stabilized zirconia sensor in a titanium flow reactor. At 400°C and 40 megapascals, the in situ pH of the fluids, ranging from 3.3 to 6.2, differs greatly from its original value of 1.9 to 7.6 at ambient conditions. The measurements agree well with theoretical predictions, showing strong associations of HCl° and NaOH° complexes in high-temperature fluids. The pH sensor provides a powerful tool to investigate unambiguously the distribution of species in aqueous fluids at elevated temperatures and pressures.

The pH of hydrothermal fluids is a critical factor in assessing homogeneous and heterogeneous chemical reactions that occur in high-temperature aqueous solutions. Thus, direct pH measurement of chemically complex aqueous fluids at supercritical conditions (*1*) has long been a major challenge (*2*). At present, in situ pH is often indirectly estimated from pH measurement at ambient conditions (for example, $pH_{25°C}$) together with available thermodynamic data. Moreover, it is typically assumed that H^+- and OH^--bearing species in fluid at high temperatures (*T*) and pressures (*P*) behave conservatively with cooling. This often is not the case, however, especially for metal- and sulfide-bearing fluids, such as mid-ocean–ridge hydrothermal vent fluids (*3*). Considering the important role of pH in sea-floor and sub–sea-floor hydrothermal processes (*4*), direct determination of fluid pH at elevated *T* and *P* would lead to a significant advance in our understanding of these important hydrothermal systems.

Numerous efforts have been made to develop instruments suitable for pH measurement in hydrothermal fluids. For example, hydrogen concentration cells (*5*) and palladium hydride electrodes (*6*) have been used successfully to determine pH at subcritical *T* (<320°C) and relatively low *P* (<25 MPa). A yttria-stabilized zirconia (YSZ) (ZrO_2 with 9% Y_2O_3) membrane (*7*), however, provides an alternative method for measuring pH at relatively high *T*, and some preliminary measurements of low–ionic strength, high-pH fluids have been made at supercritical aqueous conditions (*8–10*).

Although these conditions may be appropriate for some applications, many natural geochemical systems (*4*, *11*) and a wide range of industrial applications involving hydrothermal processes (*12*) are characterized by relatively high *T*, high *P*, high ionic strength, and low pH. For example, most axial hot-spring fluids are acidic, with dissolved Cl concentrations ranging from 40 to 200% of the seawater value (0.55 *m*), and have temperatures as high as ~400°C (*13*). Thus, to assess the viability of the YSZ membrane as a pH sensor in fluids with relatively high ionic strength (0.57 *m* NaCl) and low to moderate pH, we performed experiments at 400°C and 40 MPa and compared our results with theoretical predictions.

We performed experiments in a computer-controlled Ti flow reactor, which is especially resistant to corrosion by acidic NaCl-bearing fluids (*9*, *10*, *14*). An advantage of this facility is that the YSZ membrane and associated electrodes have direct access to the fluid phase at the experimental conditions, which ensures in situ measurements. Experiments commenced with the continuous flow (2 ml/min) of 0.57 *m* NaCl having $pH_{25°C}$ values between 1.9 and 7.6. We varied the pH of the source fluid by adding HCl. As the fluid flowed into the reactor, cell potential was measured with a Keithley (Cleveland, Ohio) 2001 electrometer with an input impedance of 10^{11} ohms. Uncertainties in the measurements were generally within ± 0.005 V at the 95% confidence level, which resulted in an uncertainty in $pH_{T,P\ \mathrm{meas}}$ of <0.05.

The electrochemical cell for pH determination can be described as

$$\mathrm{Ag}|\mathrm{AgCl}|\mathrm{Cl}^-, \mathrm{H}^+, \mathrm{H_2O}|\mathrm{YSZ}|\mathrm{Hg}|\mathrm{HgO} \quad (1)$$

As indicated, Ag/AgCl was used as a reference electrode (*15*), and because it was in direct contact with the test fluid, liquid junction potential was avoided. Other cell elements are described in (*9*, *10*). Cell potential $\Delta E(V)_{T,P}$ as a function of $pH_{T,P}$ can be described as

$$\Delta E(V)_{T,P} = \Delta E^\circ - \frac{2.303RT}{F}[\log a(\mathrm{Cl}^-) - \frac{1}{2}\log a(\mathrm{H_2O})] + \frac{2.303RT}{F}\mathrm{pH}_{T,P} \quad (2)$$

where ΔE° is the cell potential at standard state, which can be calculated from the standard state potentials of $E^\circ_{Ag/AgCl}$ and $E^\circ_{Hg/HgO}$; *R* is the gas constant; *F* is the Faraday constant; and $a(Cl^-)$ and $a(H_2O)$ are the activities of Cl^- and H_2O, respectively. Because the amount of HCl added to the test solution was negligible compared with the total amount of NaCl, the difference of the first two terms on the right side of Eq. 2 can be taken as a constant. In effect, changes in $pH_{T,P}$ are reflected solely by changes in measured $\Delta E(V)_{T,P}$. Thus, at

---

Department of Geology and Geophysics, University of Minnesota, Minneapolis, MN 55455, USA.

*To whom correspondence should be addressed.